RRP41L, a Putative Core Subunit of the Exosome, Plays an Important Role in Seed Germination and Early Seedling Growth in Arabidopsis[1][C][W]

Min Yang[2], Bangyue Zhang[2], Jianheng Jia, Chunxia Yan, Ayijiang Habaike, and Yuzhen Han*

State Key Laboratory of Plant Physiology and Biochemistry, College of Biological Sciences, China Agricultural University, Beijing 100193, China

In prokaryotic and eukaryotic cells, the 3′-5′-exonucleolytic decay and processing of RNAs are essential for RNA metabolism. However, the understanding of the mechanism of 3′-5′-exonucleolytic decay in plants is very limited. Here, we report the characterization of an Arabidopsis (*Arabidopsis thaliana*) transfer DNA insertional mutant that shows severe growth defects in early seedling growth, including delayed germination and cotyledon expansion, thinner yellow/pale-green leaves, and a slower growth rate. High-efficiency thermal asymmetric interlaced polymerase chain reaction analysis showed that the insertional locus was in the sixth exon of *AT4G27490*, encoding a predicted 3′-5′-exonuclease, that contained a conserved RNase phosphorolytic domain with high similarity to RRP41, designated *RRP41L*. Interestingly, we detected highly accumulated messenger RNAs (mRNAs) that encode seed storage protein and abscisic acid (ABA) biosynthesis and signaling pathway-related protein during the early growth stage in *rrp41l* mutants. The mRNA decay kinetics analysis for seed storage proteins, 9-cis-epoxycarotenoid dioxygenases, and ABA INSENSITIVEs revealed that RRP41L catalyzed the decay of these mRNAs in the cytoplasm. Consistent with these results, the *rrp41l* mutant was more sensitive to ABA in germination and root growth than wild-type plants, whereas overexpression lines of *RRP41L* were more resistant to ABA in germination and root growth than wild-type plants. RRP41L was localized to both the cytoplasm and nucleus, and *RRP41L* was preferentially expressed in seedlings. Altogether, our results showed that RRP41L plays an important role in seed germination and early seedling growth by mediating specific cytoplasmic mRNA decay in Arabidopsis.

RNA decay is an essential step in gene expression regulation that influences many aspects of development and growth. In eukaryotes, mRNA decay is normally initiated by the removal of the poly(A) tail (Couttet et al., 1997; Parker and Song, 2004) and then enters one of two decay pathways: (1) the decapping complex cleaves the 5′ cap, after which the 5′-3′-exoribonuclease, such as XRN1 in animals and yeast (*Saccharomyces cerevisiae*) and XRN4 in plants, hydrolyzes the mRNA from the 5′ end (Hsu and Stevens, 1993; Kastenmayer and Green, 2000; Garneau et al., 2007; Rymarquis et al., 2011), and (2) the mRNA decays from the 3′ end by the 3′-5′-exonuclease.

In eukaryotic cells, the 3′-5′-exonuclease can act alone to process the substrate in some cases, but the vast majority of 3′-5′-exonuclease activity is attributed to the exosome, which is an evolutionarily conserved macromolecular complex that mediates numerous reactions of 3′-5′ RNA processing/degradation and is essential for viability (Mitchell et al., 1997; Estévez et al., 2003). The structure of the exosome has been determined in archaea and eukaryotes, with the core forming a ring-shaped structure (Büttner et al., 2005; Lorentzen et al., 2005; Liu et al., 2006). In eukaryotes, the salient feature of the ring is defined by three distinct heterodimers of six RNase phosphorolytic (PH) domain-type proteins, MTR3-RRP42, RRP41-RRP45, and RRP43-RRP46 (Lehner and Sanderson, 2004; Hernández et al., 2006; Liu et al., 2006). However, the six-protein ring is not stable on its own in vitro and requires three subunits that contain S1 and KH domains (RRP4 links RRP41 and RRP42, RRP40 links RRP45 and RRP46, and CSL4 contacts MTR3 and RRP43) to form a stable core complex (Liu et al., 2006). In yeast, the loss of any individual subunit of the nine-component conserved core is lethal, resulting in similar ribosomal RNA (rRNA) processing defect profiles (Allmang et al., 1999a, 1999b). Moreover, x-ray crystallographic analysis of the human exosome revealed that all of its core subunits are required for its integrity (Liu et al., 2006). Using tandem affinity purification tagging in Arabidopsis (*Arabidopsis thaliana*) transgenic lines that expressed tagged versions of RRP4 and RRP41, Chekanova et al. (2007) first purified and characterized the exosome complex and revealed that the plant exosome complex contains six RNase PH domain-containing proteins and three S1 and/or KH domain proteins. Although the composition

[1] This work was supported by the National Natural Science Foundation of China (grant nos. 30670192 and 31070259).

[2] These authors contributed equally to the article.

* Corresponding author; e-mail hanyuzhen@cau.edu.cn.

The author responsible for distribution of materials integral to the findings presented in this article in accordance with the policy described in the Instructions for Authors (www.plantphysiol.org) is: Yuzhen Han (hanyuzhen@cau.edu.cn).

[C] Some figures in this article are displayed in color online but in black and white in the print edition.

[W] The online version of this article contains Web-only data.

www.plantphysiol.org/cgi/doi/10.1104/pp.112.206706

and structure of the plant exosome is similar to other eukaryotes, the function of individual subunits of the exosome appears to be different in Arabidopsis. Down-regulation of distinct subunits of the core complex results in different defects in plant development and RNA-processing profiles. For example, *csl4* null mutant plants did not manifest any obvious phenotype, and the null mutation affected only a subset of exosome targets (Chekanova et al., 2007). Therefore, the CSL4 subunit appears to be nonessential for exosome function in Arabidopsis. However, the CSL4 subunit is essential for viability in yeast (Baker et al., 1998; Allmang et al., 1999b). In contrast, the *rrp4* mutant shows seed arrest during early stages of embryonic development. RRP41 was shown to be essential for the development of female gametophytes, and homozygous *rrp41* is lethal (Chekanova et al., 2007). Additionally, RRP45 is encoded by duplicate genes: *RRP45A* and *RRP45B*. Arabidopsis single mutants that lack either RRP45A or RRP45B have no phenotype or only a mild one, respectively, whereas simultaneous down-regulation of both proteins is lethal (Hooker et al., 2007). These data indicate that subunits of the Arabidopsis exosome core complex have specialized roles in plant growth and development and make unequal contributions to the activity of the exosome in vivo. However, the functions of other predicted core subunits of the exosome, with the exception of those mentioned above, are still unclear in Arabidopsis.

Here, we report the characterization of an Arabidopsis transfer DNA (T-DNA) insertional mutant that displays severe defects in early seedling growth. High-efficiency thermal asymmetric interlaced (hiTAIL)-PCR analysis revealed that the insertional locus was in the sixth exon of *AT4G27490*, encoding a predicted 3′-5′-exonuclease that contained a conserved RNase PH domain. A previous study presumed that AT4G27490 was one subunit of the core exosome in Arabidopsis, a homolog of yeast Mtr3 (Chekanova et al., 2007), but another study suggested that it was a homolog of yeast Rrp41 (Zimmer et al., 2008). Here, we refer to AT4G27490 as RRP41L. Interestingly, we detected highly accumulated mRNAs that encode seed storage protein (SSP) and abscisic acid (ABA) biosynthesis and signaling pathway-related protein during the early growth stage in the *rrp41l* mutant. The mRNA decay kinetics analysis for SSPs, 9-cis-epoxycarotenoid dioxygenases (NCEDs), and ABA INSENSITIVEs (ABIs) revealed that RRP41L catalyzed the decay of these mRNAs in the cytoplasm. Consistent with these results, the *rrp41l* mutant was more sensitive in seed germination and root growth than wild-type plants, whereas the overexpression (*OE*) lines of *RRP41L* were more resistant to ABA in seed germination and root growth than wild-type plants. RRP41L is localized to both the cytoplasm and nucleus, and *RRP41L* is preferentially expressed in seedlings. Collectively, our results showed that RRP41L plays an important role in seed germination and early seedling growth by mediating specific cytoplasmic mRNA decay in Arabidopsis.

RESULTS

Isolation of the *slower growth* Mutant

We identified a T-DNA insertional mutant from approximately 10,000 individual T2 Arabidopsis plants, derived from approximately 1,000 T1 parents transformed with the T-DNA of *Agrobacterium tumefaciens* binary vector pCAMBIA 1300, based on its extremely slow growth phenotype, designated *slower growth* (*slg*; Fig. 1A). To genetically characterize the mutant, the *slg* line was backcrossed with the wild-type parent (ecotype Columbia). The seed germination and growth of F1 progeny appeared to be normal, similar to wild-type plants. The F2 progeny from the self-pollinated F1 showed a segregation of the *slg* phenotype of 44 to 127, corresponding to segregation of approximately one to three ($\chi^2 = 0.049$, $P > 0.05$) on Murashige and Skoog (MS) medium with hygromycin. The seedlings showing resistance to hygromycin and a slow-growth phenotype were homozygous for the T-DNA, determined by PCR (data not shown). The seedlings showing resistance to hygromycin and normal morphology, similar to wild-type plants, were heterozygous (data not shown). These data suggest that the *slg* mutant was recessive and segregated as a single nuclear locus linked to the hygromycin resistance marker.

Cloning of the *SLG* Gene

To identify the corresponding *SLG* gene, we performed hiTAIL-PCR for the T-DNA insertion site (Liu and Chen, 2007). The sequencing of the hiTAIL-PCR products suggested that the T-DNA was inserted 1,287 bp downstream of the start codon in the sixth exon of *AT4G27490* (Fig. 1B). The gene included seven introns and seven exons and encoded a 256-amino acid protein (Fig. 1B). It was predicted to be a 3′-5′-exonuclease with a conserved RNase PH domain. The Arabidopsis genome has 10 predicted RNase PH-containing proteins (Zimmer et al., 2008). Semiquantitative reverse transcription (RT)-PCR indicated that *slg* was a transcript-truncated mutant (Fig. 1C). The PCR analysis using primers specific for T-DNA and the genomic DNA indicated that all of the seedlings that displayed a slow-growth phenotype were homozygous (data not shown). In previous studies, AT4G27490 was thought to be one core subunit of the exosome, a homolog of yeast Mtr3 (Chekanova et al., 2007) or Rrp41 (Zimmer et al., 2008). We performed further phylogenetic analysis of the 10 Arabidopsis RNase PH domain-containing proteins and yeast Rrp41p and Mtr3p. The results showed that SLG was most closely related to yeast Rrp41p (Fig. 1D). Multiple gene alignment analysis showed that SLG shared 29% identity and 49% similarity with Arabidopsis RRP41 (AT3G61620; Supplemental Fig. S1). Thus, SLG was renamed RRP41-LIKE (RRP41L), and the mutant was renamed *rrp41l* accordingly.

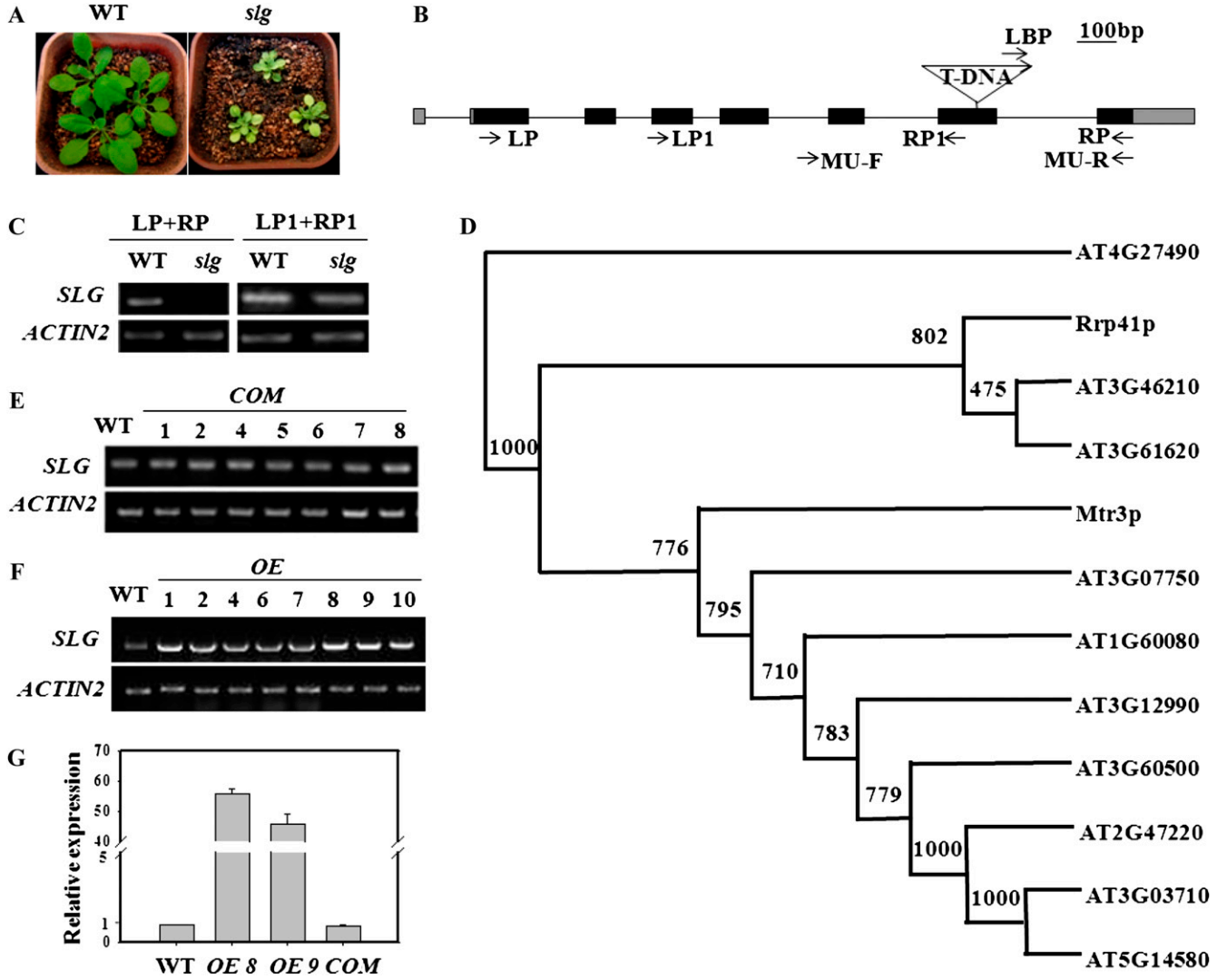

Figure 1. Identification of the *slg* mutant and characterization of the *SLG* gene. A, Four-week-old wild-type (WT) and *slg* seedlings. B, Gene structure of *SLG* and the T-DNA insertion. 5′ and 3′ untranslated regions (gray boxes); exons (black boxes); introns (black lines). LP/RP and LP1/RP1 indicate primers used to validate the transcription levels of *SLG*, and MU-F, MU-R, and LBP indicate primers used to validate the homozygous background. C, RT-PCR analysis of *SLG* transcript levels in *slg* mutants compared with corresponding wild-type plants with cDNA as the template using the primer pairs LP/RP and LP1/RP1. *ACTIN2* primers were used for PCR as an internal control. Twenty-five cycles were performed for *ACTIN2*, and 30 cycles were performed for *SLG*. As shown in A, the primer pair LP/RP spans the T-DNA insertion, whereas the primer pair LP1/RP1 is located upstream of the T-DNA insertion. D, Bootstrapped maximum parsimony tree of RNase PH domain-containing exosome proteins from Arabidopsis and yeast (Mtr3p, Rrp41p). Bootstrap support on the top of each branch, depicting how confident a branch is, was inferred from 1,000 replicates. E and F, Expression of *SLG* in different *OE* and *COM* lines analyzed by RT-PCR using the primer pair LP/RP with cDNA as the template. *ACTIN2* primers were used for PCR as an internal control. Twenty-five cycles were performed for *ACTIN2*, and 27 cycles were performed for *SLG*. G, Expression of *SLG* in *OE8*, *OE9*, and *COM* lines analyzed by qRT-PCR. [See online article for color version of this figure.]

The *rrp41l* Mutant Displays Delayed Germination and Various Developmental Defects in Early Development

The homozygous *rrp41l* T-DNA insertion mutant was characterized in detail. Under normal conditions, the *rrp41l* mutant displayed various defects in early development. The seed germination of *rrp41l* occurred later than in wild-type plants, and the difference was most distinct 36 h after the end of stratification. No obvious distinction was observed, and the germination percentages of all types of seeds were greater than 98% after 60 h (Fig. 2A). The cotyledons of the *rrp41l* mutant expanded slowly and often accumulated anthocyanins around their margins (Fig. 2, B–D).

The *rrp41l* mutant also displayed yellow-green cotyledons and pale-green early-stage rosette leaves (Fig. 2B). Consistent with this phenotype, we found a significant

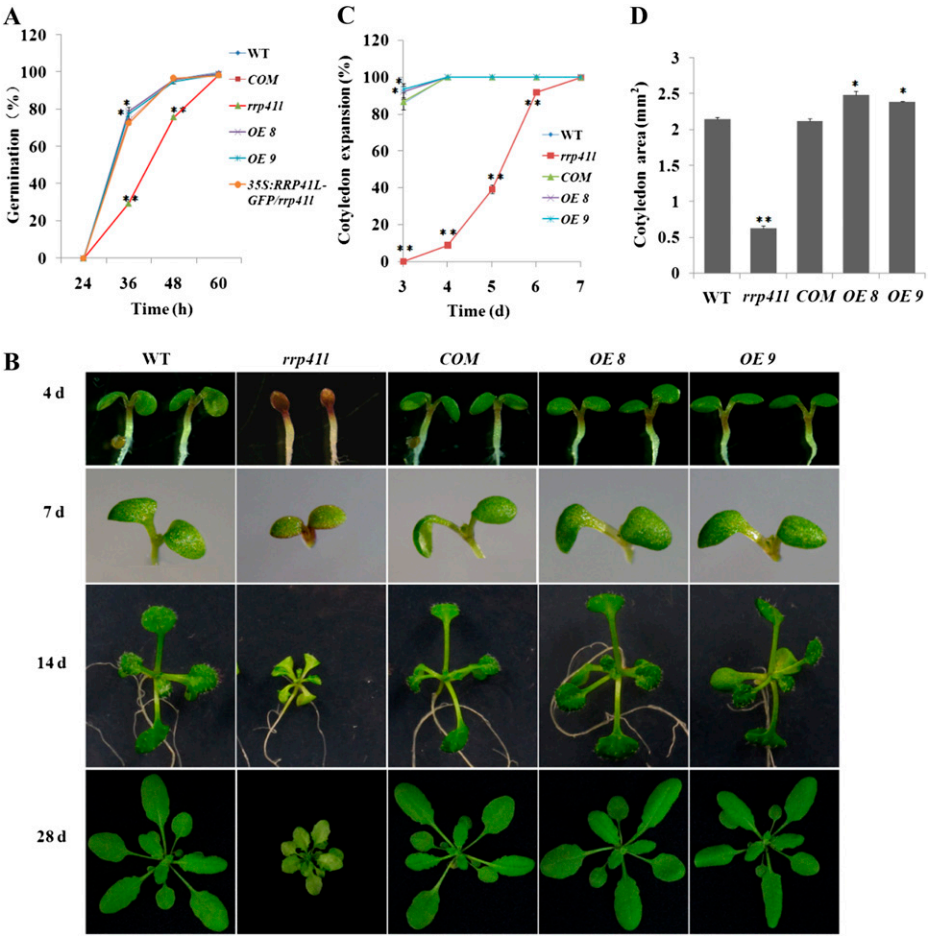

Figure 2. Phenotype characterization of wild-type (WT), *rrp41l*, *COM*, *OE8*, and *OE9* plants. A, Statistical analysis of seed germination. Data shown are means ± SD of three replicates. At least 100 seeds per genotype were scored in each replicate. B, Morphological traits of 4-, 7-, 14-, and 28-d-old seedlings. C, Percentage of cotyledon expansion (i.e. cotyledon fully opening). D, Cotyledon area of 7-d-old seedlings. The data are expressed as means ± SD of three replicates. At least 30 seedlings per genotype were measured in each replicate. All of the plants were homozygous for the mutations shown. $*P < 0.05$ and $**P < 0.01$ (Student's *t* test) indicate significant differences between mutant (or transgenic) lines and wild-type plants. [See online article for color version of this figure.]

reduction of chlorophyll content in one to six rosette leaves from 4-week-old *rrp41l* mutant plants compared with wild-type plants (Table I). The chlorophyll content of wild-type leaves was 1,051.77 ± 27.60 $\mu g\ g^{-1}$ fresh weight, whereas the chlorophyll content in *rrp41l* was reduced by nearly 50%, with only 669.40 ± 17.28 $\mu g\ g^{-1}$ fresh weight. The chlorophyll *a*/*b* ratio was reduced from 3.16 in wild-type plants to 2.56 in *rrp41l*. Additionally, in *rrp41l*, leaf size and thickness were reduced (Fig. 3, A–C), the petiole was shorter (Fig. 3, A and D), and the leaf margins displayed deep serrations (Fig. 3, A and E) compared with wild-type plants. The *rrp41l* mutant grew more slowly than wild-type plants, especially during the early stage of development. After bolting, the development of the mutant gradually recovered and finally was only shorter than wild-type plants (Supplemental Fig. S2).

We further analyzed internal leaf anatomy using light microscopy. A reduced density and irregular shape of mesophyll cells were observed in the *rrp41l* mutant, making the distinction between the palisade and spongy layers difficult (Fig. 4A). The leaves of the *rrp41l* mutant were also thinner. Further transmission electron microscopy showed that the chloroplast size and ultrastructure in the *rrp41l* mutant appeared normal, similar to wild-type plants (Supplemental Fig. S3). Scanning electron microscopy showed the details of the adaxial surface epidermises (Fig. 4, B and C) in the wild-type and *rrp41l* mutant leaves. The surface of *rrp41l* was completely crumpled, and the epidermal cells were irregularly shaped in the *rrp41l* mutant.

To confirm unequivocally that disruption of the *RRP41L* gene indeed resulted in all of the phenotypic alterations observed in the mutant, we introduced a

Table I. *Chlorophyll content of rosette leaves 1 to 6 of wild-type, COM, rrp41l, OE8, and OE9 plants*

Total chlorophyll was obtained from 100 mg of rosette leaves 1 to 6 of 4-week-old wild-type, *rrp41l*, *COM*, *OE8*, and *OE9* plants. The ratio of chlorophyll *a* to chlorophyll *b* was calculated by spectrophotometric quantification. Values shown are $\mu g\ g^{-1}$ fresh weight. Data shown are means ± SD of three independent biological determinations.

Chlorophyll	Wild Type	*rrp411*	*COM*	*OE8*	*OE9*
Total chlorophyll	1,051.77 ± 27.6	669.40 ± 17.28	1,054.03 ± 14.3	1,073.60 ± 17.09	1,044.02 ± 16.93
Chlorophyll *a*/*b* ratio	3.16 ± 0.03	2.56 ± 0.10	3.12 ± 0.06	3.21 ± 0.06	3.17 ± 0.03

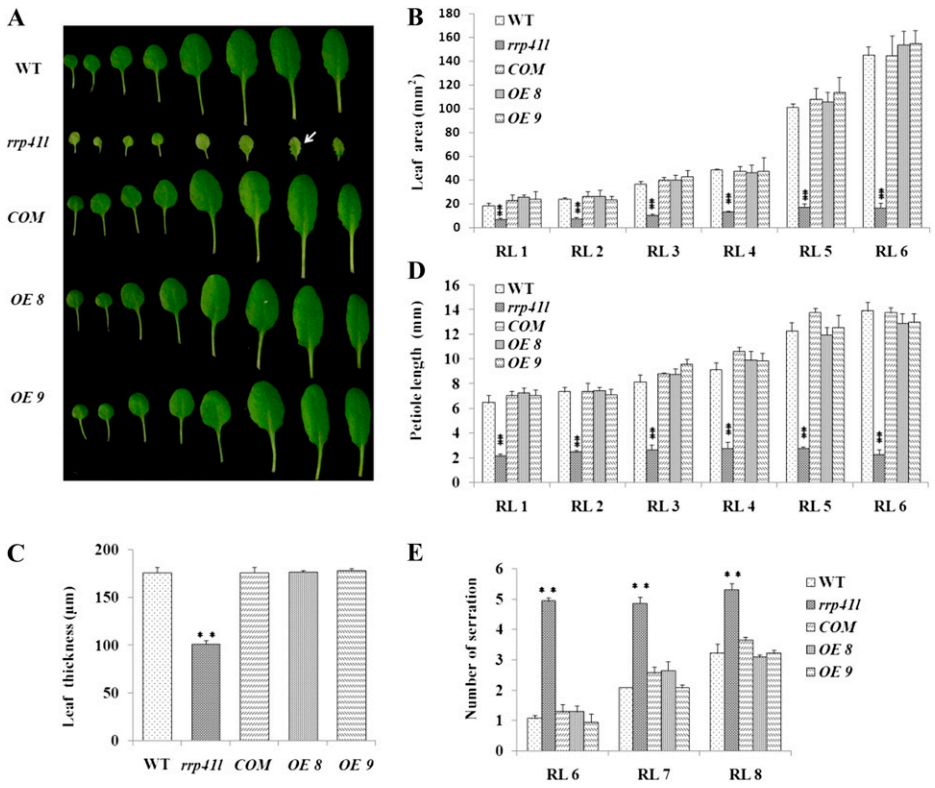

Figure 3. Comparison of rosette leaves of 4-week-old wild-type (WT), *rrp41l*, *COM*, *OE8*, and *OE9* seedlings. A, Morphological traits of rosette leaves 1 to 8. The white arrow shows the serration of *rrp41l* rosette leaves. B, Analysis of the area of rosette leaves (RL) 1 to 6. C, Thickness of the fifth rosette leaf. D, Analysis of petiole length. E, Analysis of serrations of rosette leaves 6 to 8. The data are expressed as means ± SD of three replicates. At least 30 seedlings per genotype were measured in each replicate. $*P < 0.05$ and $**P < 0.01$ (Student's *t* test) indicate significant differences between mutant (or transgenic) lines and wild-type plants. [See online article for color version of this figure.]

2,707-bp DNA fragment that included the genomic fragment of *AT4G27490* and 864-bp sequences upstream from the initiation codon into the homozygote (*rrp41l*/*rrp41l*) for genetic complementation. A total of seven complementation (*COM*) lines were generated, and transcripts were detected by RT-PCR (Fig. 1E). All *COM* lines exhibited normal morphology, similar to wild-type plants. *COM* line 7 was selected for further analysis (Figs. 1G and 2–4). We also measured the concentration of chlorophyll in the leaves of *COM* plants, which was nearly equal to wild-type plants (Table I). Altogether, these data indicate that the disruption of

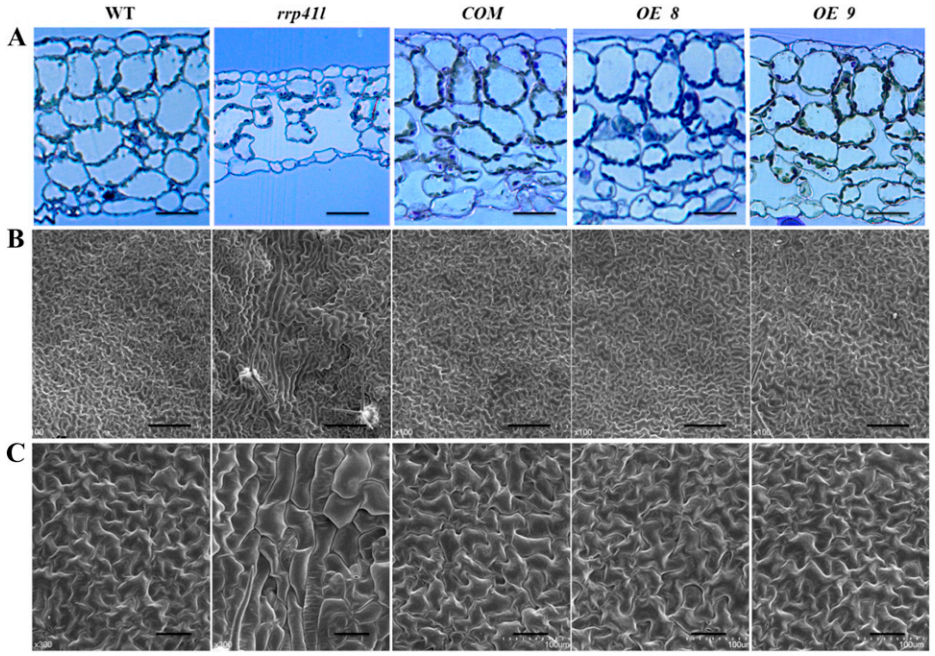

Figure 4. Anatomical structure and ultrastructure of wild-type (WT), *rrp41l*, *COM*, *OE8*, and *OE9* rosette leaves. A, Semithin section of the fifth rosette leaves. Bars = 20 μm. B, Scanning electron micrographs of the adaxial surface of the fifth rosette leaves. Bars = 200 μm. C, Micrographs show the details of their adaxial epidermises. Bars = 50 μm. [See online article for color version of this figure.]

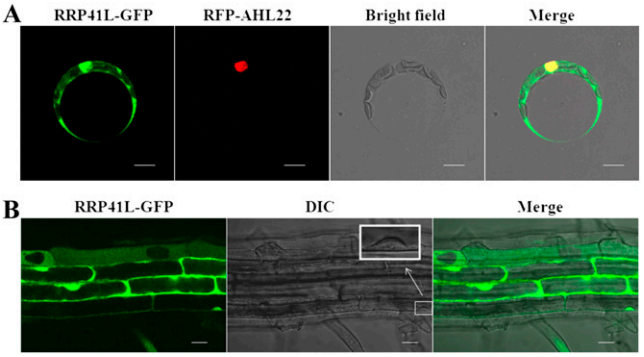

Figure 5. Subcellular localization of the RRP41L-GFP protein. A, Intracellular distribution of RRP41L-GFP and RFP-AHL22 proteins in living Arabidopsis protoplasts. Bars = 10 μm. B, Intracellular distribution of RRP41L-GFP proteins in root cells of 6-d-old stable Arabidopsis transformants. The arrow indicates the nucleus of the root cell. DIC, Differential interference contrast. Bars = 20 μm.

AT4G27490 was responsible for the *rrp41l* mutant phenotype.

Simultaneously, we generated a construct harboring *AT4G27490* complementary DNA (cDNA) under the control of the cauliflower mosaic virus 35S promoter. Seven homozygous transgenic *OE* lines were obtained, and their *RRP41L* transcript levels were detected by RT-PCR (Fig. 1F). Two lines, *OE8* and *OE9*, were selected for further analysis (Fig. 1G). Under normal conditions, *OE8* and *OE9* displayed slightly but significantly faster seed germination and cotyledon expansion than wild-type plants (Fig. 2). No obvious difference was observed in the rosette leaf size and morphology (Figs. 2B and 3), anatomic structure and ultrastructure (Fig. 4), chlorophyll content (Table I), and plant stature (Supplemental Fig. S2) in the later growth stage between the *OE* lines and wild-type plants.

RRP41L Is Localized to Both the Cytoplasm and Nucleus, and *RRP41L* Is Preferentially Expressed in Seedlings

To investigate the intracellular distribution of RRP41L, we constructed an RRP41L-GFP fusion protein expressed under the control of a cauliflower mosaic virus 35S promoter, which rescued the *rrp41l* mutant phenotype in our experiment (Supplemental Fig. S2). RRP41L-GFP and red fluorescent protein (RFP)-AHL22, an AT-rich DNA sequence (AT)-hook motif nucleus-localized protein (Xiao et al., 2009), were transiently coexpressed in living Arabidopsis protoplasts. We found that the RRP41L-GFP fusion protein was localized to both the cytoplasm and nucleus, in contrast to the nuclear distribution of RFP-AHL22 (Fig. 5A). Consistent localization was shown in the 6-d-old root cells of stable Arabidopsis transformants (Fig. 5B).

To visualize the temporal and spatial expression patterns of *RRP41L* in plant tissue, a 1,643-bp promoter fragment of *RRP41L* was fused with the *GUS* gene to generate transgenic plants. Fifteen independent transgenic lines were obtained, and more than six lines were stained and observed. GUS activity was detected in all of the organs, with the exception of the stems (Fig. 6, A–F). Interestingly, we found strong activity in imbibed seeds and seedlings (Fig. 6, A–C). However, barely detectable GUS activity was found in later rosette leaves in 4-week-old plants (Fig. 6E). A similar expression pattern was observed in six independent

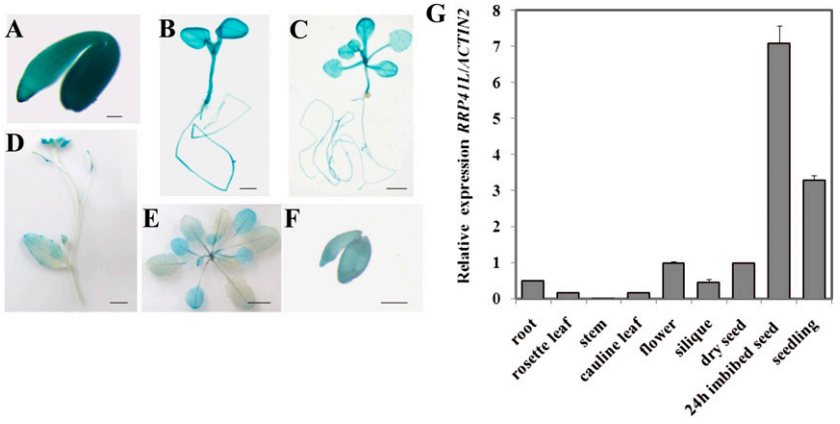

Figure 6. Expression pattern of *RRP41L*. A to F, *RRP41L* promoter activity was determined by staining Arabidopsis transformants that express the GUS reporter gene under the control of a 1,643-bp genomic sequence that contained the putative *RRP41L* promoter. A, Twenty-four-hour imbibed seed. Bar = 0.1 mm. B, Seven-day-old seedlings. Bar = 1 mm. C, Fourteen-day-old seedlings. Bar = 5 mm. D, Five-week-old plants. Bar = 0.5 mm. E, Four-week-old seedlings. Bar = 5 mm. F, Dry seeds. Bar = 0.5 mm. G, Expression of *RRP41L* in various organs determined by qRT-PCR. Total RNA was isolated from 7-d-old seedlings, dry seeds, 24-h imbibed seeds, and the roots, rosette leaves, cauline leaves, stems, flowers, and siliques of 5-week-old wild-type plants. Transcript levels were quantified by qRT-PCR against *ACTIN2*. The data are expressed as means ± SD of three independent biological determinations.

Table II. *The levels of transcripts that encode proteins related to seed maturation, photosynthesis, starch synthesis, and the GA signaling pathway in wild-type, COM, rrp41l, and OE8 seedlings*

qRT-PCR analysis of transcripts (shown in fold change) in 4-d-old wild-type, *rrp41l*, *COM*, and *OE8* seedlings is shown. The expression level in the wild type was set at 1.0. The means of three replicates of qRT-PCR and SD values are shown. Similar results were obtained when qRT-PCR was performed using a second set of samples. Dashes indicate transcripts that were not detected.

Arabidopsis Genome Initiative No.	Symbol	Wild Type	*rrp41l*	*COM*	*OE8*	Description
Transcripts encoding SSPs						
AT4G25140	OLEO1	1	12.32 ± 0.24	1.05 ± 0.07	0.81 ± 0.02	Oleosin
AT5G40420	OLEO2	1	2.18 ± 0.38	–	–	Oleosin
AT5G51210	OLEO3	1	71.06 ± 3.59	0.89 ± 0.03	0.73 ± 0.02	Oleosin
AT3G27660	OLEO4	1	14.67 ± 0.91	1.12 ± 0.01	0.96 ± 0.02	Oleosin
AT2G25890	OLEO1L	1	82.76 ± 1.24	1.01 ± 0.05	0.14 ± 0.001	Oleosin
AT3G01570	OLEO2L	1	67.88 ± 1.54	1.18 ± 0.17	0.38 ± 0.04	Oleosin
AT4G27140		1	2.42 ± 0.02	–	–	2S seed storage protein1
AT4G27150		1	0.42 ± 0.01	–	–	2S seed storage protein2
AT4G27160		1	1.01 ± 0.04	–	–	2S seed storage protein3
AT4G27170		1	5.42 ± 0.24	0.93 ± 0.06	0.36 ± 0.01	2S seed storage protein4
AT5G44120	CRA1	1	18.59 ± 0.52	1.11 ± 0.02	0.80 ± 0.09	12S seed storage protein
AT1G03890	CRA1L	1	4.17 ± 0.28	–	–	12S seed storage protein
AT1G03880	CRB	1	4.89 ± 0.60	1.00 ± 0.07	0.13 ± 0.01	12S seed storage protein
AT4G28520	CRC	1	4.22 ± 0.23	–	–	12S seed storage protein
AT1G32560		1	76.09 ± 3.93	0.94 ± 0.07	1.11 ± 0.02	Late embryogenesis abundant
AT2G35300		1	114.72 ± 3.22	0.86 ± 0.01	0.43 ± 0.01	Late embryogenesis abundant
AT1G48130		1	9.09 ± 0.33	–	–	Rehydrin
AT2G41260		1	5.56 ± 0.39	–	–	Late embryogenesis abundant
AT3G17520		1	209.44 ± 11.36	0.97 ± 0.07	0.97 ± 0.07	Late embryogenesis abundant
AT3G15670		1	353.94 ± 2.51	0.82 ± 0.01	0.82 ± 0.01	Late embryogenesis abundant
Transcripts encoding proteins related to photosynthesis and starch synthesis						
ATCG00020	PSBA	1	0.77 ± 0.02	1.08 ± 0.05	1.01 ± 0.02	PSII reaction center protein A
ATCG00490	RBCL	1	1.12 ± 0.07	1.01 ± 0.02	1.19 ± 0.02	Large subunit of Rubisco
ATCG00340	PSAB	1	0.85 ± 0.04	1.07 ± 0.05	0.83 ± 0.06	D1 subunit of PSI reaction centers
ATMG00070	NAD9	1	1.65 ± 0.06	1.24 ± 0.03	0.90 ± 0.05	NADH dehydrogenase subunit9
ATCG00120	ATPA	1	1.05 ± 0.02	1.30 ± 0.03	0.86 ± 0.02	ATPase α-subunit
AT5G46110	TPT	1	0.82 ± 0.03	0.92 ± 0.05	0.91 ± 0.08	Triose phosphate translocator
AT5G48300	ADG1	1	1.13 ± 0.04	0.86 ± 0.01	0.74 ± 0.04	ADP Glc pyrophosphorylase1
AT5G19220	ADG2	1	0.67 ± 0.04	1.16 ± 0.07	0.93 ± 0.04	ADP Glc pyrophosphorylase2
Transcripts encoding proteins related to the GA signaling pathway						
AT1G15550	GA3ox1	1	0.78 ± 0.04	1.29 ± 0.06	0.95 ± 0.06	Gibberellin 3-oxidase1
AT1G80340	GA3ox2	1	1.75 ± 0.08	1.01 ± 0.04	0.75 ± 0.02	Gibberellin-3-oxidase2
AT4G25420	GA20oxl	1	0.64 ± 0.04	1.04 ± 0.06	1.26 ± 0.10	Gibberellin 20-oxidase1
AT5G51810	GA20ox2	1	1.02 ± 0.02	1.22 ± 0.04	1.34 ± 0.03	Gibberellin 20-oxidase2
AT5G07200	GA20ox3	1	2.21 ± 0.09	0.97 ± 0.04	0.73 ± 0.05	Gibberellin 20-oxidase3
AT3G03450	RGL2	1	1.51 ± 0.05	0.98 ± 0.03	0.99 ± 0.03	RGA-like2
AT1G14920	GAI	1	1.08 ± 0.13	1.02 ± 0.06	1.05 ± 0.005	Gibberellic acid insensitive

lines. Consistent results were obtained by quantitative reverse transcription (qRT)-PCR (Fig. 6G). Overall, these data show that *RRP41L* is preferentially expressed in early-stage seedlings.

RRP41L Functions in Cytoplasmic mRNA Decay

Based on the *rrp41l* mutant phenotype, we examined the levels of transcripts that encode proteins related to photosynthesis, starch synthesis, seed maturation, the ABA biosynthesis and signaling pathways, and the GA biosynthesis and signaling pathways using qRT-PCR. Four-day-old *rrp41l* mutant seedlings were used because of their distinctive phenotype compared with wild-type seedlings. The results showed that the levels of the transcripts that encode photosynthetic-, starch synthesis-, and GA biosynthesis- and signaling pathway-related proteins accumulated almost normally in the *rrp41l* mutant compared with wild-type plants (Table II). However, highly accumulated mRNAs that encode SSPs were detected (Table II). We found that 18 of the 20 mRNAs tested were increased more than 2-fold in mutant compared with wild-type plants (Table II). Moreover, the mRNAs of key enzymes for ABA biosynthesis (i.e. NCED3, NCED5, NCED6, and NCED9) and ABA signaling transcription factors (i.e. ABI3 and ABI4 but not ABI5) also

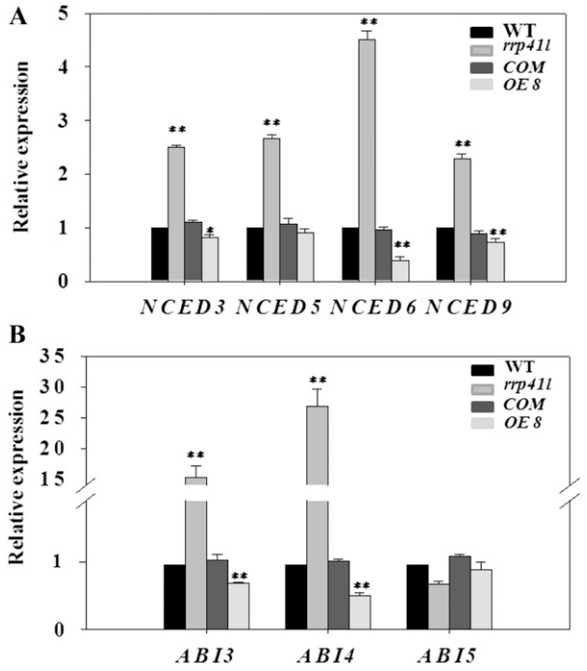

Figure 7. qRT-PCR analysis of transcripts of ABA biosynthesis and signaling-related protein genes in wild-type (WT), *rrp41l*, *COM*, and *OE8* seedlings. A, Transcription levels of mRNAs related to ABA biosynthesis proteins. B, Transcription levels of mRNAs related to ABA signaling proteins. Four-day-old seedlings were used for RNA extraction. Transcript levels were quantified by qRT-PCR against *ACTIN2*. The data are expressed as means ± SD of three independent biological determinations. $*P < 0.05$ and $**P < 0.01$ (Student's *t* test) indicate significant differences between mutant (or transgenic) lines and wild-type plants.

accumulated in *rrp41l* mutants (Fig. 7), suggesting that ABA levels and signaling could be enhanced in *rrp41l*. Consistent with these results, slight or moderate decreases in the transcript levels of most of the SSPs tested (Table II), NCED3, NCED6, NCED 9 (Fig. 7A), ABI3, and ABI4 (Fig. 7B) were detected in the *OE8* line. No significant difference was detected in the *COM* line (Fig. 7; Table II).

RRP41L has been predicted to have 3′-5′-exoribonuclease activity and to catalyze RNA decay. Therefore, we analyzed the in vivo decay kinetics of six mRNAs for AT3G15670 (a LEA protein), CRA1, NCED5, NCED6, ABI3, and ABI4 that accumulate in *rrp41l*. Four-day-old seedlings were treated with cordycepin, a drug that confers strong transcription blockade (Zhang et al., 2010), and qRT-PCR was performed. We found that the decay of AT3G15670, CRA1, NCED5, and NCED6 mRNAs was strongly diminished but not completely stopped in *rrp41l* (Fig. 8, A–D), suggesting that these mRNAs are substrates for RRP41L, but they must also be substrates for other RNA decay pathways. ABI3 and ABI4 mRNA decay was almost undetectable in *rrp41l* compared with wild-type plants (Fig. 8, E and F), suggesting that RRP41L is the only pathway for this mRNA decay during early seedling growth. The decay of AT3G15670, CRA1, NCED5, NCED6, ABI3, and ABI4 mRNAs was faster in the *OE8* line than in wild-type plants (Fig. 8). No obvious difference was observed in the *COM* line (Fig. 8).

The *rrp41l* Mutant Displayed Hypersensitivity to ABA in Seed Germination and Root Growth

Since the mRNAs of ABA biosynthesis and signaling pathway-related proteins were highly accumulated during the early growth stage in *rrp41l*, we examined the response of the *rrp41l* mutant and *OE* lines to ABA. As expected, the *rrp41l* mutant was more sensitive to ABA in seed germination (Fig. 9A), cotyledon greening (Fig. 9, B and C), and root growth (Fig. 9, B and D) than wild-type plants. In contrast to *rrp41l*, the *OE* lines were more resistant to ABA in seed germination, cotyledon greening, and root growth compared with wild-type plants (Fig. 9). These results further confirmed the role of RRP41L in the regulation of ABA synthesis and/or signaling.

RRP41L and *RRP41* Mutations Affect mRNA Levels of Different Genes

RRP41L shares 29% identity and 49% similarity with RRP41 (AT3G61620) in Arabidopsis, and they are all closely related to yeast Rrp41p (Fig. 1D; Supplemental Fig. S1). Chekanova et al. (2007) identified 266 up-regulated mRNAs in $rrp41^{iRNAi}$ (for estradiol-inducible RNA interference-mediated knockdown of *RRP41*) using tiling arrays. To investigate whether mutations in *RRP41L* and *RRP41* affect common mRNAs, we randomly chose 16 mRNAs from the 266 mRNAs that were identified to be up-regulated in the $rrp41^{iRNAi}$ mutant and examined their transcript levels in *rrp41l* using qRT-PCR. The results showed only slight increases or decreases in these mRNA levels compared with wild-type plants (Fig. 10). We also compared the up-regulated mRNAs in *rrp41l* examined by qRT-PCR, with 266 mRNAs revealed using tiling arrays in the $rrp41^{iRNAi}$ mutant (Chekanova et al., 2007). No mRNA overlap was found, with the exception of *OLEO2* (Supplemental Table S1). These data suggest that RRP41L and RRP41 function distinctively, and thus RRP41 and RRP41L mutations result in different phenotypes.

DISCUSSION

RRP41L Is Essential for Seed Germination and Early Seedling Growth in Arabidopsis

In this study, we characterized an Arabidopsis *rrp41l* mutant that displays severe defects in early seedling growth, including delayed germination and cotyledon expansion, thinner and yellow/pale-green

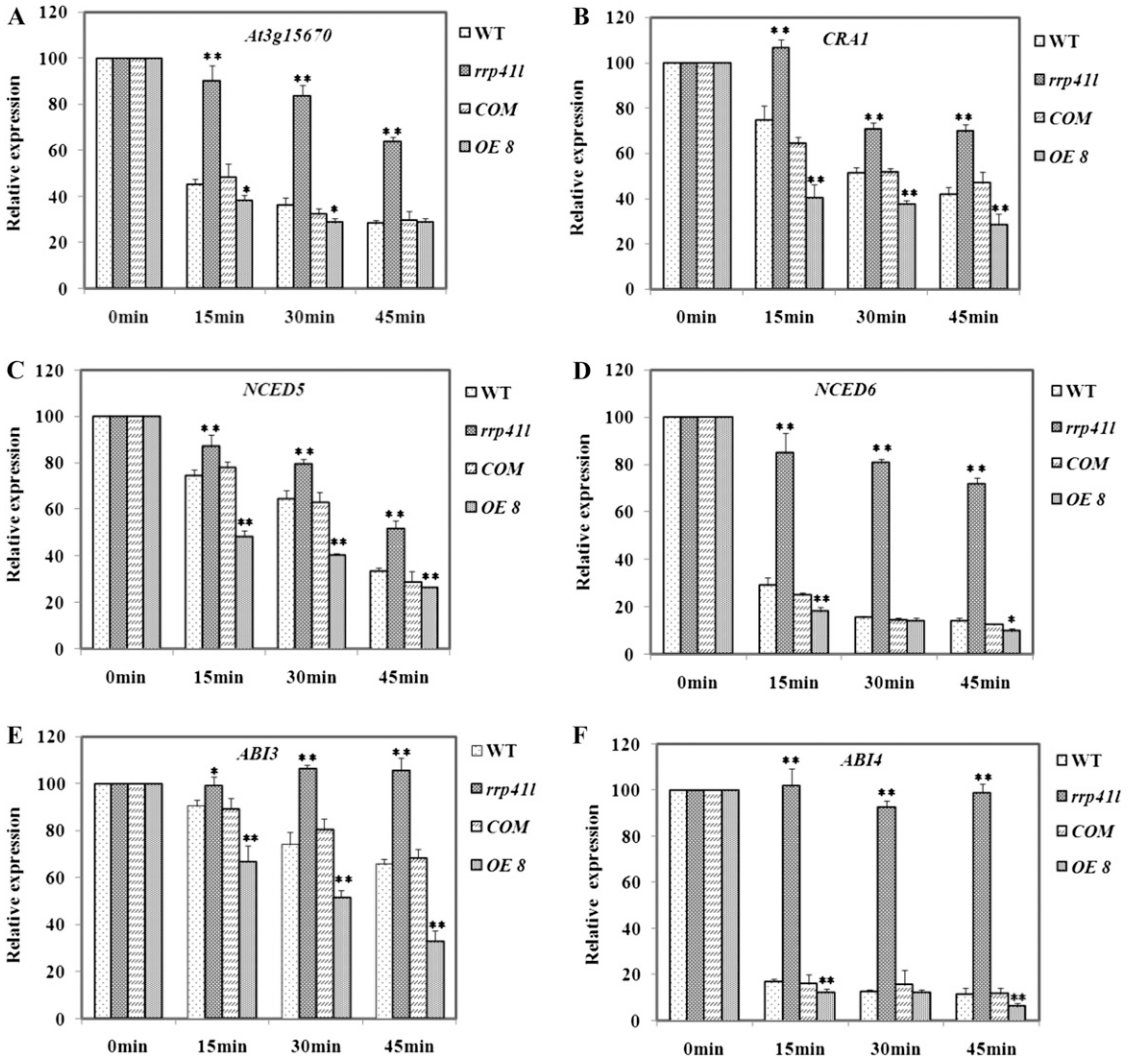

Figure 8. RNA decay comparison of six mRNAs in wild-type (WT), *rrp41l*, *COM*, and *OE8* seedlings using qRT-PCR. Relative expression is shown for *AT3G15670*, which encodes a LEA protein (A), *CRA1* (B), *NCED5* (C), *NCED6* (D), *ABI3* (E), and *ABI4* (F) in wild-type, *rrp41l*, *COM*, and *OE8* seedlings before the addition of cordycepin (0 min) and 15, 30, and 45 min after the addition of cordycepin. Four-day-old seedlings were used for treatment and then for RNA extraction. Transcript levels were quantified by qRT-PCR against *ACTIN2*. The data are expressed as means ± SD of three independent biological determinations. $*P < 0.05$ and $**P < 0.01$ (Student's *t* test) indicate significant differences between mutant (or transgenic) lines and wild-type plants.

leaves, and slower early growth than wild-type plants (Fig. 2). After bolting, the growth and development of the mutant gradually recovered and was finally only shorter than wild-type plants (Supplemental Fig. S2). Consistent with its phenotype, expression profile analysis revealed that *RRP41L* was preferentially expressed in imbibed seeds and seedlings (Fig. 6, A–C and G). These results suggest that RRP41L plays an important role in seed germination and early seedling development in Arabidopsis. It should be pointed out that *rrp41l* is a transcript-truncated mutant. Although the T-DNA insertion site is located in the PH domain (Supplemental Fig. S1), it has not been shown whether *rrp41l* is a null mutant. So it could not been excluded that null mutants of *RRP41L* have more severe phenotypes.

We further found that the transcript levels of ABA biosynthesis key enzymes, ABA signaling transcription factors, and SSPs were all highly accumulated during early seedling growth in the *rrp41l* mutant. NCED constitutes a key step in the regulation of ABA biosynthesis. For example, *NCED3* together with *NCED5* promotes ABA production, affecting plant growth and water stress tolerance (Frey et al., 2012). NCED6 and NCED9 are also required for ABA biosynthesis during seed development (Lefebvre et al., 2006). The high accumulation of these mRNAs suggests that ABA levels may be increased in *rrp41l*. ABI3, ABI4, and ABI5 are transcription factors that function in a combinatorial network and act to positively regulate the ABA signaling pathway (Söderman et al.,

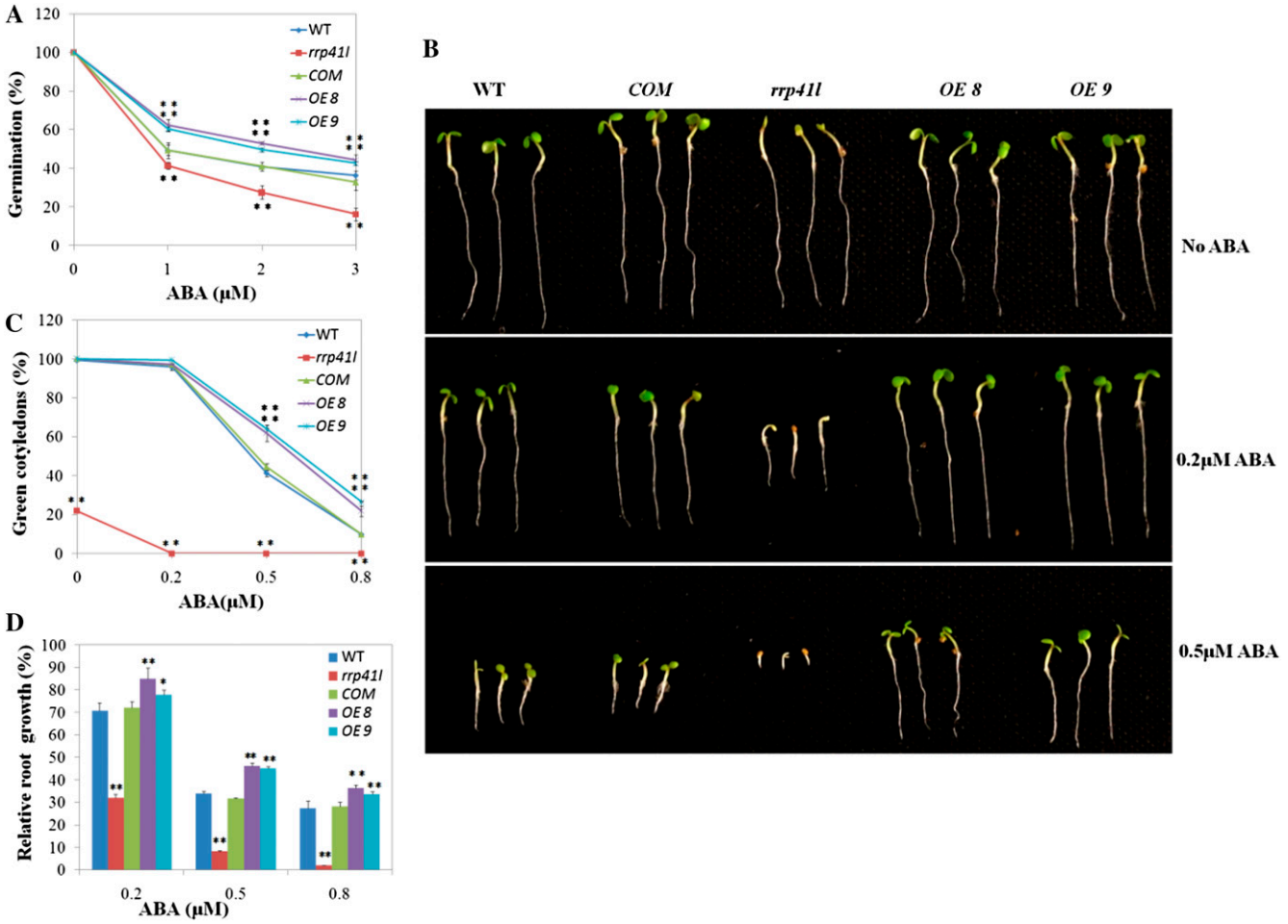

Figure 9. ABA responses of wild-type (WT), *rrp41l*, *COM*, *OE8*, and *OE9* plants in seed germination and postgermination growth. A, The germination percentage of seeds grown on MS medium with different concentrations of ABA was recorded 3 d after the end of stratification. The data are expressed as means ± SD of three replicates. At least 100 seeds per genotype were measured in each replicate. B, Seedlings on medium with different concentrations of ABA 5 d after the end of stratification. C, Analysis of cotyledon greening 5 d after the end of stratification. The data are expressed as means ± SD of three replicates. At least 100 seeds per genotype were measured in each replicate. D, Analysis of seedling root length. Root length was measured 5 d after the end of stratification. Relative root growth compared with that on ABA-free medium is indicated. The data are expressed as means ± SD of three replicates. At least 30 seedlings per genotype were measured in each replicate. $*P < 0.05$ and $**P < 0.01$ (Student's *t* test) indicate significant differences between mutant (or transgenic) lines and wild-type plants. [See online article for color version of this figure.]

2000). ABI3 is necessary for the expression of numerous late embryogenesis genes that are thought to be essential for the acquisition of desiccation tolerance (Parcy et al., 1994; Parcy and Giraudat, 1997). ABI4 is a repressor of lipid breakdown that regulates seed germination in Arabidopsis (Penfield et al., 2006). The accumulation of these mRNAs for ABA biosynthesis and signaling may explain the delayed germination and slower growth phenotypes of *rrp41l*. ABI5 acts downstream of ABI3 in the same pathway to regulate a subset of late embryogenesis-abundant genes during both developmental stages (Finkelstein and Lynch, 2000; Lopez-Molina et al., 2002), but ABI5 mRNA changes little in *rrp41l*. Additionally, we also found that SSP mRNAs were highly accumulated in *rrp41l*. SSPs are well known to be expressed during the maturation phase of embryogenesis, but when seed dormancy is broken, these proteins decrease rapidly, followed by germination (Parcy et al., 1994; Lopez-Molina et al., 2002), cotyledon expansion, greening, and finally vegetative growth. Thus, the accumulation of SSP mRNAs in *rrp41l* may also contribute to delayed germination and slower seedling growth.

To further confirm the role of RRP41L, we overexpressed *RRP41L* using a 35S promoter in wild-type plants. Slightly faster germination and cotyledon expansion were observed under normal growth conditions (Fig. 2). The transcript assay (Fig. 7; Table II) and mRNA decay assay (Fig. 8) also revealed slight or moderate decreases in ABI and SSP transcripts in the *OE* line compared with wild-type plants, consistent with their phenotypes. Interestingly, compared with

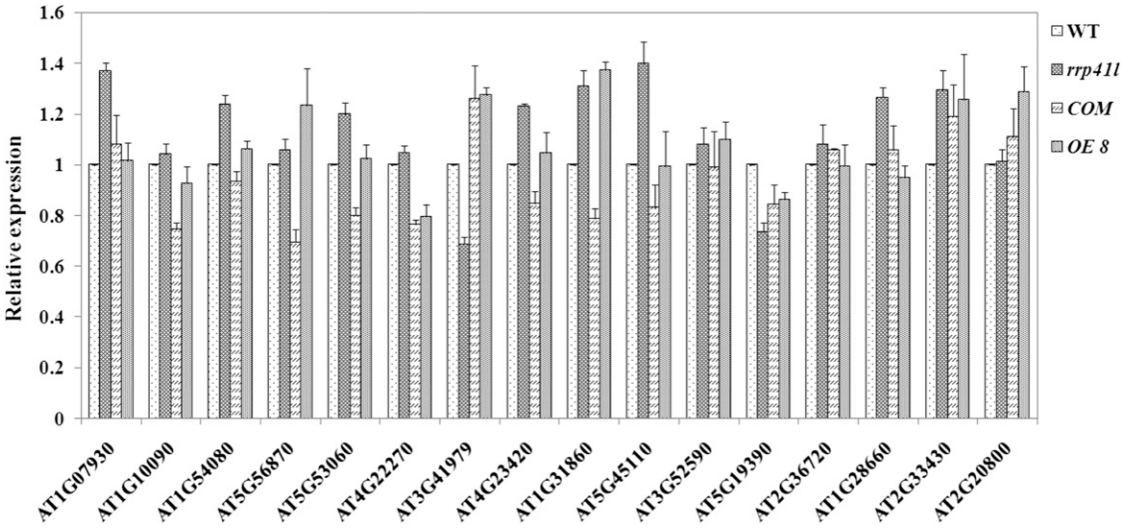

Figure 10. Transcription levels of mRNAs that were up-regulated in *rrp41*^{iRNAi} mutant in wild-type (WT), *COM*, *rrp41l*, and *OE8* seedlings by qRT-PCR. Four-day-old seedlings were used for RNA extraction. Transcript levels were quantified by qRT-PCR against *ACTIN2*. The data are expressed as means ± SD of three independent biological determinations.

OE lines grown on a standard medium, *OE* lines grown on a medium with ABA displayed more obvious increases in germination, cotyledon greening (expansion), and root growth compared with wild-type plants (Fig. 9). The expression of ABIs and SSPs is induced by ABA (Finkelstein et al., 2002; Gutierrez et al., 2007); therefore, an overdose of RRP41L may be more required for seed germination and seedling growth under ABA treatment. Conversely, the *rrp41l* mutant displayed hypersensitivity to ABA in seed germination and root growth (Fig. 9). These results suggest that RRP41L regulated seed germination and early development by down-regulating the ABA signaling pathway.

In addition to ABA, the GA signaling pathway also plays an important role in seed germination (Finkelstein et al., 2008). We examined the levels of the transcripts that encode the key enzymes of GA biosynthesis, GA3ox1, GA3ox2, GA20ox1, GA20ox2, and GA20ox3, and the GA signaling factors GAI and RGL2 (Yamaguchi, 2008). GA20ox catalyzes C_{19}-GA formation from C_{20}-GA. GA3ox catalyzes the final step in the formation of the biologically active product. GAI and RGL2, members of the DELLA subfamily of GRAS proteins, play negative regulatory roles in the GA signaling pathway. No obvious changes were detected in these transcripts in *rrp41l* or the *OE* line (Table II). These results suggest that RRP41L affects seed germination largely independent of the GA signaling pathway.

RRP41L Functions in Specific Cytoplasmic mRNA Decay

In Arabidopsis, *RRP41L* was predicted to encode a 256-amino acid protein with a conserved RNase PH domain that has 3′-5′-exoribonuclease activity and is involved in RNA processing. In this study, we provided evidence that RRP41L functions in cytoplasmic mRNA decay. We examined the transcription levels of *AT3G15670* that encode a LEA protein, *CRA1*, *NCED5*, *NCED6*, *ABI3*, and *ABI4* in 4-d-old seedlings treated with cordycepin. In wild-type plants, these mRNA levels decreased rapidly after the addition of cordycepin. However, in the *rrp41l* mutant, these mRNA levels decreased modestly (Fig. 8, A–D) or were nearly unchanged (Fig. 8, E and F) under the same conditions. These results indicate that the disruption of *RRP41L* function led to a defect in mRNA decay. Thus, RRP41L functions in cytoplasmic mRNA decay. The RRP41L-GFP fusion experiment showed that RRP41L was localized to the cytoplasm and nucleus (Fig. 5). This supports the hypothesis that RRP41L functions in the cytoplasm. The RRP41L localization to the nucleus suggests that it also plays a role in the nucleus. A previous study demonstrated that the nuclear exosome is able to perform the precise 3′ end processing of the 5.8S rRNA precursor (Allmang et al., 1999b) and completely degrade the external transcribed rRNA spacer (Allmang et al., 2000). However, further studies are required to elucidate the role of RRP41L in the nucleus.

In all of the mRNAs examined, only the mRNAs that encode SSP and ABA biosynthesis and signaling-related protein were highly accumulated in *rrp41l* (Fig. 7; Table II), suggesting that the decay of RNA by RRP41L is selective. Moreover, the effects of the RRP41L mutation on the decay kinetics of the six mRNAs examined were different. After transcription was inhibited by adding cordycepin, the mRNA levels of AT3G15670, CRA1, NCED5, and NCED6 decreased, although the decay rate was much slower than in wild-type plants (Fig. 8, A–D), whereas the decay of ABI3 and ABI4 mRNA was almost completely stopped in the *rrp41l*

mutant (Fig. 8, E and F). These results suggest that the transcripts of these SSPs decayed not only via the RRP41L pathway but also via other decay pathways. Indeed, previous reports have shown that the decapping complex is involved in SSP decay in Arabidopsis (Xu et al., 2006; Xu and Chua, 2009). These data also suggest that ABI3 and ABI4 mRNA decays only through the RRP41L pathway during early seedling growth. Altogether, RRP41L appears to function in specific cytoplasmic mRNA decay in Arabidopsis.

RRP41L Is a Putative Core Subunit of the Exosome and Has Unique Functions That Are Different from Other Subunits in Arabidopsis

A previous study showed that down-regulation of individual subunits of the exosome complex led to distinct defects in Arabidopsis development (Chekanova et al., 2007). For example, a *csl4* mutant showed no obvious phenotype, and *rrp4* mutant seeds arrested at an early stage of embryo development. RRP41 was shown to be essential for the development of the female gametophyte, and a homozygous *rrp41* mutant was lethal. The *rrp45B* mutant has a reduction of cuticular wax loads on the stem and silique (Hooker et al., 2007). In our study, we showed that mutation of RRP41L, one predicted subunit of the exosome, also resulted in unique phenotypes. The *rrp41l* mutant displayed a delay in seed germination and slower growth at an early stage (Figs. 2 and 3). However, seed development and fertility were normal, similar to wild-type plants. No apparent overlap in the phenotypes of these mutants was observed. Specifically, although RRP41L shares 29% identity and 49% similarity with RRP41 (AT3G61620) in Arabidopsis, and they are all closely related to yeast Rrp41p (Fig. 1D; Supplemental Fig. S1), their phenotypes were quite different. qRT-PCR indicated that the transcript levels of 16 mRNAs that were all identified to be up-regulated in the $rrp41^{iRNAi}$ mutant were not obviously increased in *rrp41l* compared with wild-type plants (Fig. 10). Additionally, we compared the up-regulated mRNAs in *rrp41l* and $rrp41^{iRNAi}$ mutants (Chekanova et al., 2007), and no mRNA overlap was found, with the exception of OLEO2 (Supplemental Table S1). These data suggest that RRP41 and RRP41L affect mRNA levels of different genes; therefore, a disruption of their function resulted in distinct phenotypes. Overall, we suggest that RRP41L has particular functions for specific cytoplasmic mRNA decay, especially during seed germination and early seedling development in Arabidopsis.

MATERIALS AND METHODS

Plant Materials and Growth Conditions

Arabidopsis (*Arabidopsis thaliana*) ecotype Columbia was used in all of the experiments as the wild-type control. All of the plants were grown on MS medium (4.43 g of MS salts, 30 g L^{-1} Suc, and 1% [w/v] agar powder, pH 5.8) or on soil at 22°C with a 16-h-light/8-h-dark photoperiod. To analyze the relative expression of *RRP41L*, rosette leaves, cauline leaves, roots, stems, flowers, and siliques from 5-week-old plants and 7-d-old seedlings were collected for RNA isolation and qRT-PCR.

Isolation of the *slg/rrp41l* Mutant, hiTAIL-PCR, and Molecular Cloning of the *RRP41L* Gene

We used binary-vector pCAMBIA 1300 (CAMBIA) to generate the T-DNA collection. The transformed seeds were screened with MS medium that contained 25 μg mL^{-1} hygromycin. After 3 d in the dark at 4°C, the seeds were transferred to 22°C with a 16-h-light/8-h-dark photoperiod. The *slg/slg* (*rrp41l/rrp41l*) mutant was screened from approximately 10,000 seedlings from approximately 1,000 independent T1 Arabidopsis lines based on its slow-growth phenotype.

The hiTAIL-PCR procedure and arbitrary degenerate primers for pCAMBIA 1300 were described by Liu and Chen (2007). Cosegregation of the T-DNA insertion site and mutant phenotype were analyzed with LBP (5′-GAAGAGGCCCGCACCGATCGCCCTT-3′) and plant-specific primers (MU-F, 5′-GGTTCGCTTGGACATTCGTG-3′, and MU-R, 5′-CATTCATCGGAAGCTGAGGC-3′). For the homozygous mutant plants, only PCR using LBP and MU-R primers could amplify a DNA fragment of approximately 500 bp. For wild-type plants, only PCR using MU-F and MU-R could amplify an 872-bp DNA fragment. For heterozygous plants, PCR with both primer pairs showed positive results. Additionally, the primers LP/RP (LP, 5′-ATGGCAGCTAAACCTGGAGCCGCAAC-3′, and RP, 5′-TCATTCATCGGAAGCTGAGGCAGACTG-3′) and LP1/RP1 (LP1, 5′-TTTTGCTTCCCCTACTCTTGG-3′, and RP1, 5′-CTTCACATCCTTCCTCCTCTG-3′) were used to validate the transcription levels of *RRP41L* in mutant and wild-type plants.

Complementation was performed as follows. A 2,707-bp DNA fragment that included the full-length genomic DNA and 864-bp sequences upstream from the initiation codon from wild-type plants were amplified using the primers *COM*-LP (5′-CTGCAGAAATCTGAGAGTTATGGTACTAGCCACTGGGC-3′) and *COM*-RP (5′-CCATGGTCATTCATCGGAAGCTGAGGCAGACTG-3′). Following sequence verification, the fragment was cloned into a pCAMBIA 3301 binary vector. The construct was transformed into *Agrobacterium tumefaciens* strain GV3101 and then introduced into the homozygous (*rrp41l/rrp41l*) plants using the floral dip method (Clough and Bent, 1998). The transformants were screened with 519 μL L^{-1} Basta treatment. The T2/T3 transformant *COM* lines were screened with Basta, and all of the seedlings of homozygous *COM* lines were resistant to Basta and showed a green phenotype. The homozygous *COM* lines were then verified by PCR, and the following primers were used: LBP/MU-R (genomic DNA as the template), LP/RP (cDNA as the template), and *COM*-LP/*COM*-RP (genomic DNA as the template).

For the *OE* of *RRP41L*, the *RRP41L* coding sequence was PCR amplified with the primers *OE*-LP (5′-AAGCTTATGGCAGCTAAACCTGGAGCCGCAAC-3′) and *OE*-RP (5′-GGTACCTCATTCATCGGAAGCTGAGGCAGACTG-3′) using wild-type cDNA as the template. The resulting PCR product was cloned into the binary vector pSuper1300 under the control of the cauliflower mosaic virus 35S promoter. The construct was transformed into wild-type plants to obtain the transgenic plants. The T2/T3 seeds from each transgenic line were screened with MS medium that containing 25 μg mL^{-1} hygromycin.

Construction of the Phylogenetic Tree

The amino acid sequences for the RNase PH exosome subunits were aligned using the ClustalX program (Thompson et al., 1997). A maximum parsimony tree was generated using PHYLIP software (http://evolution.genetics.washington.edu/phylip/; version 3.69) with 1,000 bootstrap resampling and visualized using TreeView (http://taxonomy.zoology.gla.ac.uk/rod/treeview.html).

Phenotype Characterization and Microscopic Observations

For seed germination, plants of different genotypes were grown under the same conditions, and seeds were collected at the same time. For each comparison, seeds were planted on the same plate that contained MS medium with or without different concentrations of ABA as indicated. The plates were chilled at 4°C in the dark for 3 d (stratified) and moved to 22°C with a 16-h-light/8-h-dark photoperiod. The percentage of seed germination was scored at

the indicated times. Germination was defined as the obvious emergence of the radicle through the seed coat. The germination results were calculated based on at least three independent experiments. At least 100 seeds for each genotype were scored for each replicate. To study the effect of ABA on post-germination growth, the seeds were sown on a medium that contained different concentrations of ABA as indicated. The percentage of cotyledon greening was recorded 5 d after the end of stratification. Cotyledon greening is defined as obvious cotyledon expansion and turning green. The length of primary roots was measured using a ruler. The results were calculated based on at least three independent experiments. At least 30 seedlings for each genotype were scored for each replicate.

For leaf morphology observation, 4-d-old seedlings were observed using a microscope (Olympus SZX16-DP72), and 7-d-old seedlings were photographed with a Canon digital camera (PowerShot G12). For histological analysis, the fifth rosette leaves from 4-week-old wild-type and *rrp41l* plants were fixed in formaldehyde/glutaraldehyde fixative (1% [v/v] glutaraldehyde and 4% [w/v] paraformaldehyde in 0.05 mol L^{-1} phosphate buffer, pH 7.2). After fixation, the tissues were dehydrated in ethanol and then embedded in Spurr's resin (SPI-CHEM). Thin sections (approximately 2 μm) were prepared using a microtome (Leica EM UC7), stained with 0.5% (w/v) crystal violet, and then observed by light microscopy (ZEISS Scope A1). Additionally, specimens were sliced to yield ultrathin sections (LKB-8800) and stained with uranyl acetate and alkaline lead citrate before being examined with a transmission electron microscope (JEM-123O). For scanning electron microscopy, plant material was prepared as described by Serrano-Cartagena et al. (2000). Micrographs were taken in a scanning electron microscope (Hitachi S-3400N).

Chlorophyll Content Analysis

Chlorophyll was extracted from the leaves and measured according to the protocol of Grbić and Bleecker (1995). Extracts were obtained from 100 mg of fresh tissue from one to six rosette leaves from 4-week-old plants and homogenized in 4 mL of 80% (v/v) acetone. Spectrophotometric quantification was performed in a Beckman DUR650 spectrophotometer. Pigment measurements were repeated in three independent experiments.

RNA Isolation and qRT-PCR Analysis

Total RNA from plants of different genotypes was isolated using TRI reagent (Invitrogen), and cDNA was synthesized using an oligo$(dT)_{18}$ primer with the Promega RT system. We performed qRT-PCR using TaKaRa SYBR Premix Ex Taq and the ABI 7500 Real Time PCR system. *ACTIN2* amplification was used as an internal control. Each qRT-PCR analysis used a minimum of three biological replicates and two technical replicates. The primers for qRT-PCR are shown in Supplemental Table S2. Some primer sequences were taken from Xu and Chua (2009), Seo et al. (2004), and Jiang et al. (2012).

RNA Decay Analysis

RNA decay assays were performed as described by Gutiérrez et al. (2002). Four-day-old wild-type, *rrp41l*, *COM*, and *OE8* seedlings were collected, pretreated for 30 min with incubation buffer with gentle shaking at 160 rpm on an orbital shaker at 22°C, and then supplied with cordycepin (Sigma) to a final concentration of 1 mM. The samples were collected before the addition of cordycepin, referred to as 0 min, and then the seedlings were collected after the addition of cordycepin at 15, 30, and 45 min (160 rpm at 22°C). The sample for each time point was frozen in liquid nitrogen immediately and stored at −80°C. The samples were then used for RNA isolation and qRT-PCR.

Subcellular Localization of RRP41L-Fused GFP Protein

To express the RRP41L-GFP fusion protein under the control of the 35S promoter, the full-length coding sequence without the TGA stop codon was cloned from the cDNA of wild-type plants with the following primers: FU-LP (5′-AAGCTTATGGCAGCTAAACCTGGAGCCGCAAC-3′) and FU-RP (5′-GGTACCTTCATCGGAAGCTGAGGCAGACTG-3′). The coding sequence was fused to the pSuper 1300-GFP vector, in which GFP is tagged at the C terminus. The plasmids were transformed into Arabidopsis protoplasts to observe the transient expression of the fusion protein. The protoplast isolation and plasmid transformation procedures were described by Kim and Somers (2010). The stable Arabidopsis transformants were obtained using the floral dip method, and transgenic plants were selected on MS plates that contained 25 mg L^{-1} hygromycin. The GFP and RFP fluorescence of the transgenic protoplasts and the GFP fluorescence of the transgenic plants were observed using a Zeiss 510 META confocal laser scanning microscope. To confirm that the localization of RRP41L was unaffected by GFP fusion, the 35S:RRP41L-GFP plasmids were transformed into the *rrp41l*/*rrp41l* mutant. Nine homozygous transgenic *35S:RRP41L-GFP/rrp41l* lines were obtained.

Assay of GUS Activity

For the histochemical analysis of GUS staining, the *RRP41L* promoter:GUS gene was constructed using PCR amplification of a fragment 1,643 bp upstream from the initial codon of *RRP41L* using the primers PRO-LP (5′-CCAAGCTTTAAAGAGCCTTCTCATATGTG-3′) and PRO-RP (5′-CCGGATCCTGTTCTGAGCTGAGACTAAAC-3′); the fragment was then cloned into a pCAMBIA 1391 vector. Transformation was performed as described above. The tissues were examined using a microscope (Olympus SZX16-DP72), and digital images were recorded with a Canon digital camera (PowerShot G12).

Supplemental Data

The following materials are available in the online version of this article.

Supplemental Figure S1. Alignment of amino acid sequences of RNase PH domain-containing exosome proteins from Arabidopsis and yeast.

Supplemental Figure S2. Development of wild-type, *rrp41l*, *COM*, *OE8*, *OE9* and *35S:RRP41L-GFP/rrp41l* plants after bolting.

Supplemental Figure S3. Transmission electron micrographs of chloroplasts in wild-type, *rrp41l*, *COM*, *OE8*, and *OE9* plants.

Supplemental Table S1. Comparison of up-regulated mRNAs in *rrp41l* mutant and $rrp41^{iRNAi}$ mutant.

Supplemental Table S2. Primers used for qRT-PCR.

ACKNOWLEDGMENTS

We thank Prof. Shuhua Yang for technical assistance in protoplast isolation and critical reading of the manuscript, Prof. Ziding Zhang and Dr. Yuan Zhou for the analysis of the phylogenetic tree, and Prof. Yongfu Fu for providing the RFP-AHL22 plasmid.

Received September 1, 2012; accepted November 1, 2012; published November 6, 2012.

LITERATURE CITED

Allmang C, Kufel J, Chanfreau G, Mitchell P, Petfalski E, Tollervey D (1999a) Functions of the exosome in rRNA, snoRNA and snRNA synthesis. EMBO J **18:** 5399–5410

Allmang C, Mitchell P, Petfalski E, Tollervey D (2000) Degradation of ribosomal RNA precursors by the exosome. Nucleic Acids Res **28:** 1684–1691

Allmang C, Petfalski E, Podtelejnikov A, Mann M, Tollervey D, Mitchell P (1999b) The yeast exosome and human PM-Scl are related complexes of 3′→5′ exonucleases. Genes Dev **13:** 2148–2158

Baker RE, Harris K, Zhang K (1998) Mutations synthetically lethal with cep1 target S. cerevisiae kinetochore components. Genetics **149:** 73–85

Büttner K, Wenig K, Hopfner KP (2005) Structural framework for the mechanism of archaeal exosomes in RNA processing. Mol Cell **20:** 461–471

Chekanova JA, Gregory BD, Reverdatto SV, Chen H, Kumar R, Hooker T, Yazaki J, Li P, Skiba N, Peng Q, et al (2007) Genome-wide high-resolution mapping of exosome substrates reveals hidden features in the Arabidopsis transcriptome. Cell **131:** 1340–1353

Clough SJ, Bent AF (1998) Floral dip: a simplified method for Agrobacterium-mediated transformation of Arabidopsis thaliana. Plant J **16:** 735–743

Couttet P, Fromont-Racine M, Steel D, Pictet R, Grange T (1997) Messenger RNA deadenylylation precedes decapping in mammalian cells. Proc Natl Acad Sci USA **94:** 5628–5633

Estévez AM, Lehner B, Sanderson CM, Ruppert T, Clayton C (2003) The roles of intersubunit interactions in exosome stability. J Biol Chem **278:** 34943–34951

Finkelstein R, Reeves W, Ariizumi T, Steber C (2008) Molecular aspects of seed dormancy. Annu Rev Plant Biol **59:** 387–415

Finkelstein RR, Gampala SSL, Rock CD (2002) Abscisic acid signaling in seeds and seedlings. Plant Cell (Suppl) **14:** S15–S45

Finkelstein RR, Lynch TJ (2000) The *Arabidopsis* abscisic acid response gene *ABI5* encodes a basic leucine zipper transcription factor. Plant Cell **12:** 599–609

Frey A, Effroy D, Lefebvre V, Seo M, Perreau F, Berger A, Sechet J, To A, North HM, Marion-Poll A (2012) Epoxycarotenoid cleavage by NCED5 fine-tunes ABA accumulation and affects seed dormancy and drought tolerance with other NCED family members. Plant J **70:** 501–512

Garneau NL, Wilusz J, Wilusz CJ (2007) The highways and byways of mRNA decay. Nat Rev Mol Cell Biol **8:** 113–126

Grbić V, Bleecker AB (1995) Ethylene regulates the timing of leaf senescence in Arabidopsis. Plant J **8:** 595–602

Gutierrez L, Van Wuytswinkel O, Castelain M, Bellini C (2007) Combined networks regulating seed maturation. Trends Plant Sci **12:** 294–300

Gutiérrez RA, Ewing RM, Cherry JM, Green PJ (2002) Identification of unstable transcripts in Arabidopsis by cDNA microarray analysis: rapid decay is associated with a group of touch- and specific clock-controlled genes. Proc Natl Acad Sci USA **99:** 11513–11518

Hernández H, Dziembowski A, Taverner T, Séraphin B, Robinson CV (2006) Subunit architecture of multimeric complexes isolated directly from cells. EMBO Rep **7:** 605–610

Hooker TS, Lam P, Zheng H, Kunst L (2007) A core subunit of the RNA-processing/degrading exosome specifically influences cuticular wax biosynthesis in *Arabidopsis*. Plant Cell **19:** 904–913

Hsu CL, Stevens A (1993) Yeast cells lacking 5′→3′ exoribonuclease 1 contain mRNA species that are poly(A) deficient and partially lack the 5′ cap structure. Mol Cell Biol **13:** 4826–4835

Jiang S, Kumar S, Eu YJ, Jami SK, Stasolla C, Hill RD (2012) The Arabidopsis mutant, fy-1, has an ABA-insensitive germination phenotype. J Exp Bot **63:** 2693–2703

Kastenmayer JP, Green PJ (2000) Novel features of the XRN-family in Arabidopsis: evidence that AtXRN4, one of several orthologs of nuclear Xrn2p/Rat1p, functions in the cytoplasm. Proc Natl Acad Sci USA **97:** 13985–13990

Kim J, Somers DE (2010) Rapid assessment of gene function in the circadian clock using artificial microRNA in Arabidopsis mesophyll protoplasts. Plant Physiol **154:** 611–621

Lefebvre V, North H, Frey A, Sotta B, Seo M, Okamoto M, Nambara E, Marion-Poll A (2006) Functional analysis of Arabidopsis NCED6 and NCED9 genes indicates that ABA synthesized in the endosperm is involved in the induction of seed dormancy. Plant J **45:** 309–319

Lehner B, Sanderson CM (2004) A protein interaction framework for human mRNA degradation. Genome Res **14:** 1315–1323

Liu Q, Greimann JC, Lima CD (2006) Reconstitution, activities, and structure of the eukaryotic RNA exosome. Cell **127:** 1223–1237

Liu Y-G, Chen Y (2007) High-efficiency thermal asymmetric interlaced PCR for amplification of unknown flanking sequences. Biotechniques **43:** 649–656

Lopez-Molina L, Mongrand S, McLachlin DT, Chait BT, Chua NH (2002) ABI5 acts downstream of ABI3 to execute an ABA-dependent growth arrest during germination. Plant J **32:** 317–328

Lorentzen E, Walter P, Fribourg S, Evguenieva-Hackenberg E, Klug G, Conti E (2005) The archaeal exosome core is a hexameric ring structure with three catalytic subunits. Nat Struct Mol Biol **12:** 575–581

Mitchell P, Petfalski E, Shevchenko A, Mann M, Tollervey D (1997) The exosome: a conserved eukaryotic RNA processing complex containing multiple 3′→5′ exoribonucleases. Cell **91:** 457–466

Parcy F, Giraudat J (1997) Interactions between the ABI1 and the ectopically expressed ABI3 genes in controlling abscisic acid responses in Arabidopsis vegetative tissues. Plant J **11:** 693–702

Parcy F, Valon C, Raynal M, Gaubier-Comella P, Delseny M, Giraudat J (1994) Regulation of gene expression programs during *Arabidopsis* seed development: roles of the ABI3 locus and of endogenous abscisic acid. Plant Cell **6:** 1567–1582

Parker R, Song H (2004) The enzymes and control of eukaryotic mRNA turnover. Nat Struct Mol Biol **11:** 121–127

Penfield S, Li Y, Gilday AD, Graham S, Graham IA (2006) *Arabidopsis* ABA INSENSITIVE4 regulates lipid mobilization in the embryo and reveals repression of seed germination by the endosperm. Plant Cell **18:** 1887–1899

Rymarquis LA, Souret FF, Green PJ (2011) Evidence that XRN4, an Arabidopsis homolog of exoribonuclease XRN1, preferentially impacts transcripts with certain sequences or in particular functional categories. RNA **17:** 501–511

Seo M, Aoki H, Koiwai H, Kamiya Y, Nambara E, Koshiba T (2004) Comparative studies on the Arabidopsis aldehyde oxidase (AAO) gene family revealed a major role of AAO3 in ABA biosynthesis in seeds. Plant Cell Physiol **45:** 1694–1703

Serrano-Cartagena J, Candela H, Robles P, Ponce MR, Pérez-Pérez JM, Piqueras P, Micol JL (2000) Genetic analysis of incurvata mutants reveals three independent genetic operations at work in Arabidopsis leaf morphogenesis. Genetics **156:** 1363–1377

Söderman EM, Brocard IM, Lynch TJ, Finkelstein RR (2000) Regulation and function of the Arabidopsis *ABA-insensitive4* gene in seed and abscisic acid response signaling networks. Plant Physiol **124:** 1752–1765

Thompson JD, Gibson TJ, Plewniak F, Jeanmougin F, Higgins DG (1997) The CLUSTAL_X Windows interface: flexible strategies for multiple sequence alignment aided by quality analysis tools. Nucleic Acids Res **25:** 4876–4882

Xiao C, Chen F, Yu X, Lin C, Fu YF (2009) Over-expression of an AT-hook gene, AHL22, delays flowering and inhibits the elongation of the hypocotyl in Arabidopsis thaliana. Plant Mol Biol **71:** 39–50

Xu J, Chua NH (2009) *Arabidopsis* decapping 5 is required for mRNA decapping, P-body formation, and translational repression during postembryonic development. Plant Cell **21:** 3270–3279

Xu J, Yang JY, Niu QW, Chua NH (2006) *Arabidopsis* DCP2, DCP1, and VARICOSE form a decapping complex required for postembryonic development. Plant Cell **18:** 3386–3398

Yamaguchi S (2008) Gibberellin metabolism and its regulation. Annu Rev Plant Biol **59:** 225–251

Zhang W, Murphy C, Sieburth LE (2010) Conserved RNaseII domain protein functions in cytoplasmic mRNA decay and suppresses Arabidopsis decapping mutant phenotypes. Proc Natl Acad Sci USA **107:** 15981–15985

Zimmer SL, Fei Z, Stern DB (2008) Genome-based analysis of Chlamydomonas reinhardtii exoribonucleases and poly(A) polymerases predicts unexpected organellar and exosomal features. Genetics **179:** 125–136